MODELING OF CORROSION IN RC STRUCTURES UNDER VARIABLE CHLORIDE ENVIRONMENT BASED ON THERMODYNAMIC ELECTRO-CHEMICAL APPROACH

Raja Rizwan HUSSAIN,[1] Tetsuya ISHIDA[2]

[1] PhD Candidate, Department of Civil Engineering, University of Tokyo, Japan

[2] Assoc. Professor, Department of Civil Engineering, University of Tokyo, Japan

***ABSTRACT*:** RC structures exposed to aggressive environments such as chloride attack suffer from accelerated corrosion of rebars. Corrosion is an electrochemical thermodynamic phenomenon influenced by several parameters and some of them are being overlooked in the past research works. The purpose of this paper is therefore, to model and verify the corrosion of reinforcement throughout the life of concrete structures by incorporating realistic electro-chemical thermodynamic models and actual field condition experimentation. The modeling task has been incorporated by the use of concrete durability model 'DuCOM' developed by our research group as a computational platform on which the chloride induced corrosion based reinforced concrete performance and quality at early age and throughout the life of concrete structure is examined in both space and time domains.

KEYWORDS: Corrosion, chloride, concrete, modeling, thermodynamic electro-chemistry.

1. INTRODUCTION

The Corrosion of steel reinforcement in concrete is of great concern in the view of safety and durability of reinforced concrete structures. Concrete is subjected to various environmental loadings throughout its service life span as shown in Figure 1. The premature deterioration of reinforced concrete member has become a major concern in many countries throughout the world.

Figure 1. Environmental Loadings on Concrete

Since steel corrosion is an electrochemical process, its rate is influenced by several factors such as amount of oxygen, chloride, carbon-dioxide, ambient temperature etc, and corrosion of steel may vary from one place to another due to the difference in seasons and environmental conditions. Therefore, it is necessary to conduct in-depth investigations in order to further understand the mechanisms of corrosion in concrete.

2. OBJECTIVES

The main objective of this paper is to investigate the severe environmental conditions especially emphasizing on the effect of chloride and temperature (Figure 2) on corrosion of reinforcing steel in concrete both by experimentation and modeling approach by clarifying the mechanisms involved therein. This eletrochemical thermodyna--mic phenomenon is influenced by several factors and some of them are being overlooked in the past research works and have difference of opinion. Also it was found that the experimental data for the

combined effect of chloride and temperature on corrosion of reinforcement especially in the higher range is limited (Nishida et al., 2005). For this purpose corrosion potential vs. chloride and temperature profiles are obtained experimentally. For the sake of further accuracy and precision gravimetric corrosion mass loss and consequent corrosion rate is also obtained by modeling and successively verified by experimentation.

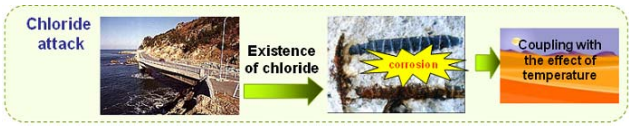

Figure 2. Coupled Effect of Chloride and Temperature on Corrosion.

3. METHODOLOGY (DuCOM)

The methodology adopted in this research is based on DuCOM, a 3D finite element model developed by our research group as a general framework for corrosion assessment and numerical analysis of RC structures subjected to severe environmental conditions. A general frame work of mass and ion equilibrium equations and an electro-chemical reaction model of corrosion in reinforced concrete has been presented by Ishida, T. (1999a). Thus the influential parameters on the theorem of corrosion process for the severe environmental effects are determined experimentally and simulated in numerical terms for the enhancement of existing model in this research. The reliability of this model is verified through comparison of simulation with experiment results.

The constituent material models employed in DuCOM are formulated based on micro-mechanical phenomena such as hydration, moisture, transport and cementitious microstructure formation. Their strong interrelationships are taken into account by real time sharing of material characteristic variables across each sub-system. The development of multi-scale micro pore structures at early age is obtained based on the average degree of cement hydration in the mixture. The non-linearity in corrosion process and severe environmental effects along with various connected sub-models (Figure 3) to acquire the parameters necessary for the computation of corrosion are taken into account automatically in the unified framework of the program.

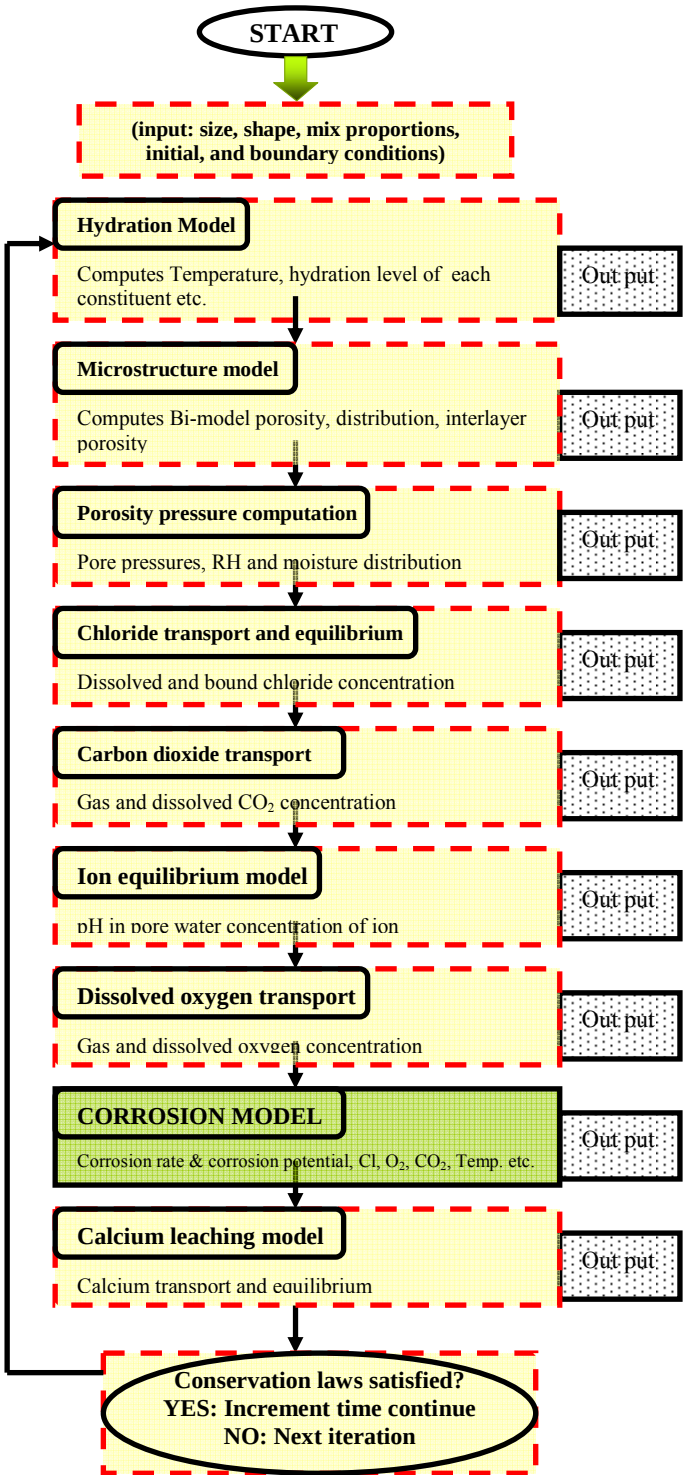

Figure 3. Unified Framework of **DuCOM**

4. NUMERICAL MODELING

4.1 Governing Laws and Equations

The corrosion model in the DuCOM system was firstly adopted from Ishida, T., 1999, Maekawa & Ishida, 2003. In the model a general scheme of micro-cell corrosion is introduced based on thermodynamic electro-chemistry. Initially, electric potential of corrosion cell is obtained from the ambient temperature, pH in pore solution and partial pressure of oxide, which are calculated by other subroutines in the system. The half-cell potential can be expressed with the Nernst Equation (1).

$$Fe(s) \longrightarrow Fe^{2+}(aq) + e(Pt)$$
$$E_{Fe} = E_{Fe}^{\Theta} + (RT/z_{Fe}\,F)\ln h_{Fe}^{2+}$$
$$O_2(g) + 2H_2O(l) + 4e(Pt) = 4OH^-(aq)$$
$$E_{02} = E_{02}^{\Theta} + ((RT/z_{02}\,F)\ln(P_{02}/P^{\Theta})\text{-}0.06pH \qquad (1)$$

Where

E_{Fe}: standard cell potential of Fe, anode (V,SHE),

E_{02}: standard cell potential of O_2, cathode (V, SHE),

E_{Fe}^{Θ}: standard cell potential of Fe at 25°C (=-0.44V),

E_{02}^{Θ}: standard cell potential of O_2 at 25°C (=0.40V),

z_{Fe}: the number of charge of Fe (=2)

z_{02}: the number of charge of O_2 (=2)

P^{Θ}: atmospheric pressure

For physical explanation of the corrosion reaction in relation to the above equations, refer to Figure 4.

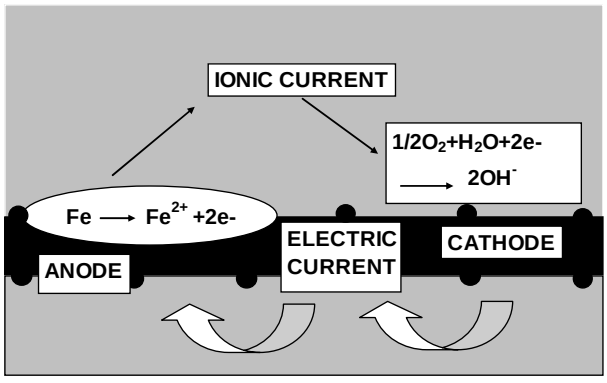

Figure 4. Physical Electro-Chemical Mechanism of Steel Reinforcement Corrosion in Concrete.

4.2 Incorporation of Tafel Diagram in the Corrosion Model

Tafel Diagram (Julius Tafel, 1906) is a useful tool for simulating the corrosion phenomenon of metals. From the electric potential and the formation of passive layers, electric current that involves chemical reaction can be calculated so that the conservation law of electric charge should be satisfied in a local area. Corrosion potential 'Ecorr.' and corrosion current 'Icorr.' can be obtained as the point of intersection of the two lines as shown in Figure 5.

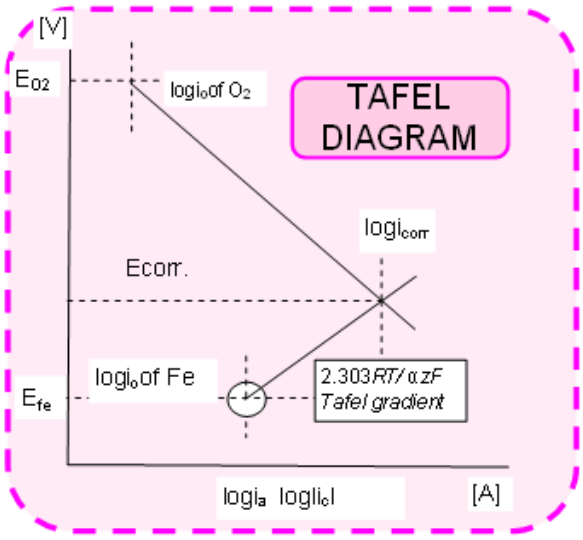

Figure 5. Corrosion Current and Corrosion Potential.

Most of the metal corrosion occurs via electrochemical reactions at the interface between the metal and an electrolyte solution. A thin film of moisture on a metal surface forms the electrolyte for atmospheric corrosion. Corrosion normally occurs at a rate determined by an equilibrium between opposing electrochemical reactions. First is the anodic reaction, in which a metal is oxidized, releasing electrons into the metal. The other is the cathodic reaction, in which a solution species (often O_2 or H^+) is reduced, removing electrons from the metal. When these two reactions are in equilibrium, the flow of electrons from each reaction is balanced, and no net electron flow (electrical current) occurs.

The two reactions can take place on one metal or on two dissimilar metals (or metal sites) that are electrically connected. Figure 6 below diagrams this process.

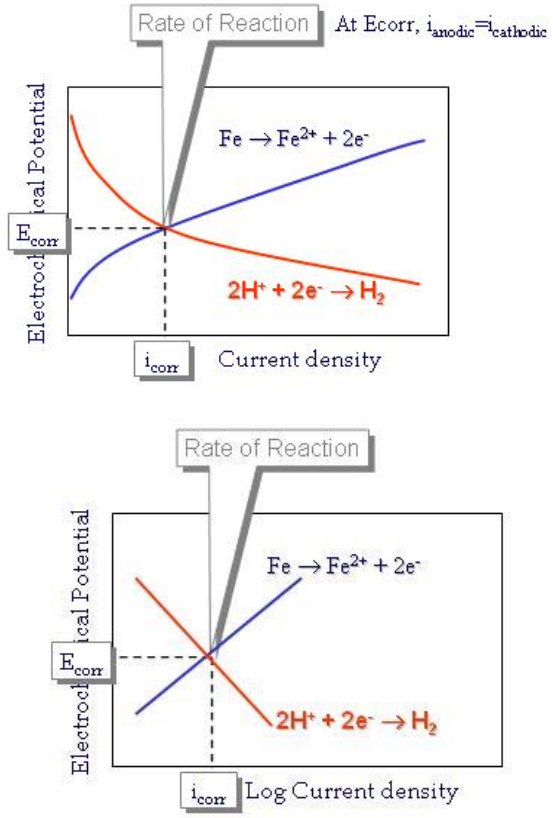

Figure 6. E-logi Corrosion Process Mechanism

The relationship of electric current and voltage for the anode and cathode can be expressed by the following Nernst Equation (2) as,

$$\eta^a = (2.303RT/0.5\ z_{Fe}\ F)\log(i_a/i_o)$$
$$\eta^c = -(2.303RT/(1-\alpha)z_{02}\ F)\log(i_c/i_o) \quad (2)$$

Where:

η^a : Overvoltage at anode [V]

η^c : Overvoltage at cathode [V]

F: Faraday's constant

i_a: Electric current density at anode [A/m^2]

i_c: Electric current density at cathode [A/m^2]

In the model i_a=1.0E-5 A/m^2, i_c=1.0E-10 A/m^2 and α=0.5.

4.3 Corrosion in Concrete and the Effect of Chloride

Although most corrosion takes place in water, corrosion in non-aqueous systems is not unknown. When it comes to the modeling of corrosion in concrete like steel reinforcement embedded in concrete under the effect of severe environment such chloride attack, then need arises to introduce some semi-empirical equations which logically satisfy the existing corrosion science laws, principals and are verified by experiments. Infact when we talk about modeling of large scale real structures, then pure theory becomes insufficient and somehow theory and practice has to be combined together in the form of a semi-empirical-theoretical approach.

The existence of passive layer reduces the corrosion progress and serves as a barrier and protective layer for steel reinforcement in concrete. For the initiation of corrosion reaction it is necessary that the passive layers must be destroyed through some means such as chloride attack. Glass and Page, 1991 reported that the effect of chloride on corrosion is an anodic controlled reaction. Therefore in this research the modeling has been accomplished by varying the anodic potential and anodic gradient. In this corrosion model the phenomenon of passive layer breaking and progress of corrosion is described by varying the anodic tafel gradient and anodic reaction potential as a function of chloride concentration.

4.3 Anodic Tafel Gradient Factor 'fp'

The effect of chloride on corrosion has been incorporated by varying the tafel gradient of anodic reaction 'ba' with free chloride concentration (C_{Cl}) as shown in Equation (3).

$$ba = (2.303RT/0.5\ z_{Fe}\ F)fp \quad (3)$$

where:

$$fp = 3.17 \times 10^{-2}\ C_{Cl}^{-0.826}$$

For further explanation of the above equation please refer to Figure 7.

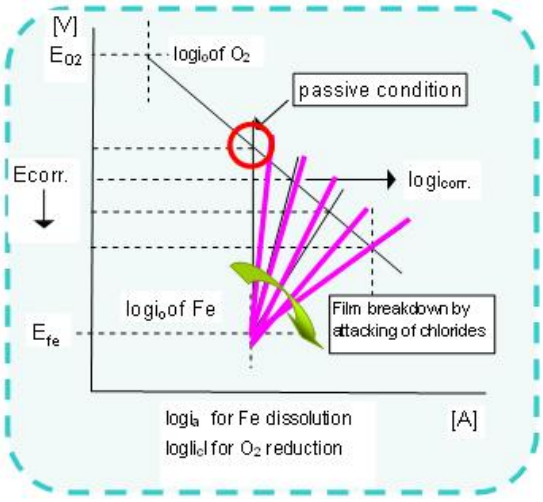

Figure 7. Potential and Current Increment by Cl Migration and Breakdown of Passive Layer.

In the model this semi-empirical-theoretical factor 'fp' accounts for the change in anodic gradient. When the chloride concentration is zero, the factor 'fp' becomes infinity and the rebar is considered to be in perfect passive condition represented by a 90° perpendicular anodic line of the tafel diagram as shown in the Figure 7. As the chloride concentration increase, the passive layer starts breaking simulated by decrease in 'fp' resulting in the fall of anodic gradient moving the point of intersection of anode and cathode lines towards the more negative corrosion potential and increase in corrosion current until the threshold chloride value is reached and the passive layer is completely destroyed. When chloride ions exist in the system, the passive region which has been occupied by Fe_3O_4 until this time will disappear. Also the protective region of Fe_2O_3 will divide into two portions. The lower layer is truly passive but the upper one is somewhat unstable due to the localized destruction and pitting (West 1986). It has been reported from the past researchers that as chlorides increase around reinforcement, current density of corrosion becomes larger due to the breakdown of passive film (Broomfield 1997). At the threshold chloride value, the passive layer is completely destroyed, thus the factor 'fp' becomes 1.0 and the gradient of anodic reaction in the tafel diagram becomes equal to the actual tafel gradient as given by Nernst equation already explained above. In the light of past research works (B. H oh (2004), BS 8110:1997, ACI Code 222R-96, Norweigian Codes, Evertte and Treadaway, 1983) the threshold chloride value has been fixed as 0.4% total chlorides by mass of cement. Since the model is based on the amount of free chloride existing in the pore water, conversion of free Cl to bound Cl and vice versa is done using chloride equilibrium Equation 4 given by Ishida and Lan Anh, 2005.

$$C_b = \frac{\alpha C_f}{1+\beta C_f} \qquad (4)$$

$$\alpha = 11.8; \beta = 4.0$$

Where:

C_f: Free chloride concentration expressed as % mass of binder.

C_b: Bound chloride concentration expressed as % mass of binder.

4.4 Anodic Potential Factor 'F_{Cl}'

Based on the fact that the chloride induced corrosion reaction is anodic controlled in nature (Glass and Page, 1991), a semi-empirical factor F_{Cl} is introduced in order to initiate anodic potential variation as a function of chloride content as shown in Equation 5.

$$E_{Fe} = E_{Fe}^{\Theta} + ((RT/z_{Fe}\,F)\ln h_{Fe}^{2+})\,F_{Cl} \qquad (5)$$

Where,

$$F_{Cl} = 1+3x10^{-3}\ln(10^4 C_{Cl}+1)+(1.2C_{Cl}/(C_{Cl}+1))$$

This factor 'F_{Cl}' shifts the anodic curve diagonally downwards with the increase in the chloride content, thus moving the point of intersection of cathode and anode polarization curves towards the more negative potential and higher corrosion current direction.

Consider Figure 8 for further illustration of the working of 'F_{Cl}'.

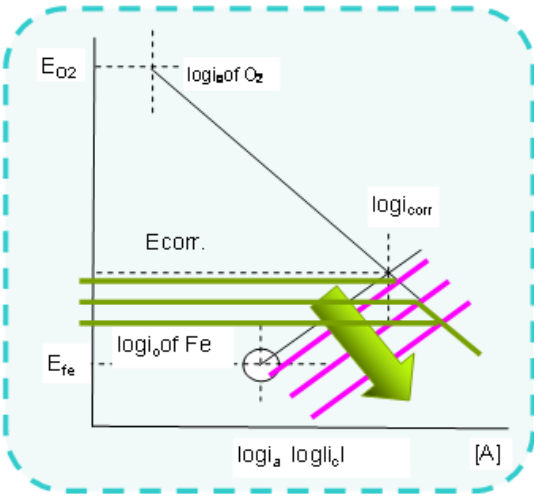

Figure 8. Illustration of Semi-Empirical Function'F_{Cl}'

In the absence of chloride the factor F_{Cl} is equal to one and the anodic potential is equal to the original anodic potential of the tafel diagram given by the Nernst equation as already explained above. As the chloride attack becomes active, the factor F_{Cl} starts increasing more than 1.0 with the increase in chloride concentration in a non linear path as shown in the Figure 9.

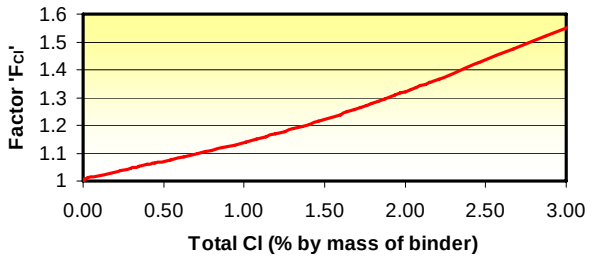

Figure 9. Anodic Potential Factor 'F_{Cl}'

The cathodic gradient 'bc' varies according to the nature of chemical reaction and the availability of oxygen near the surface of steel bar embedded in concrete. The corrosion model under discussion can limit the amount of corrosion due to the unavailability of enough amount of oxygen. But, the most common case in practical field is that the real structures hardly encounter conditions in which the concrete is completely submerged under water for very long duration enough to initiate oxygen controlled (cathodic dependent) corrosion reaction (M. Raupach, 1996). Therefore, in this study for the corrosion reaction of steel in chloride contaminated concrete, 'bc' has been semi-empirically determined as bc = 0.1405 by sensitivity analysis and has been incorporated in the corrosion model considering a free flow of oxygen. Lastly, using the Faraday's Law, electric current of corrosion is converted to the rate of steel reinforcement corrosion.

In this research the model is enhanced from the previous research (Ishida and Hussain, 2005) by combining potential and tafel slope models to execute at the same time (Figure 10) as both the tafel anodic slope and potential are influenced by chloride migration.

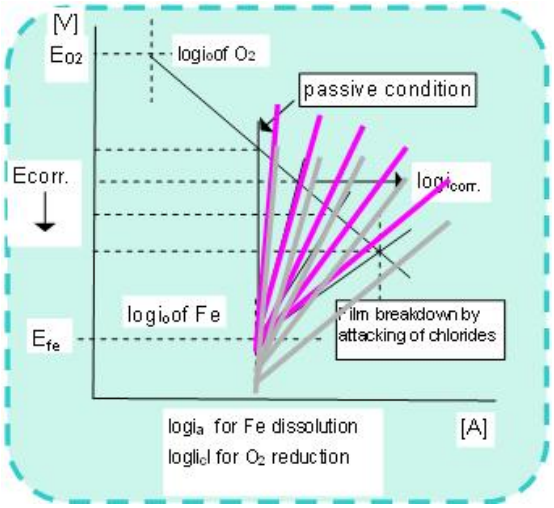

Figure 10. Coupling of 'fp' & 'F_{Cl}' in the model

4.5 Effective Corrosion Current Reduction Factor 'A_{fr}' for Saturated Area of concrete

Corrosion is an electrochemical phenomenon which requires electrolyte for the occurrence of corrosion reaction. Therefore, it is necessary to calculate the effective corrosion current in the system with reference to saturated area of concrete only as shown

in Equation (6).

$Icorr_{eff.} = Icorr.\ A_{fr,}$

$$A_{fr}=(\phi_{cp}S_{cp}+\phi_{gl}S_{gl})*(1.0-\alpha_{Vf}V_f) \quad (6)$$

Where;

ϕ_{cp} : Capillary zone porosity

S_{cp} : Saturation of capillary zone pores

ϕ_{gl} : Gel zone porosity

S_{gl} : Saturation of gel zone pores

V_f : Volume of fine aggregate

α_{Vf} : % fine aggregate present in the vicinity of rebar.

Consider Figure 11 for clarification of this function. Theoretically and numerically the saturated area depends on the capillary zone porosity, gel zone porosity and their respective degree of saturation in the aggregate free volume of concrete which is a heterogeneous material in nature.

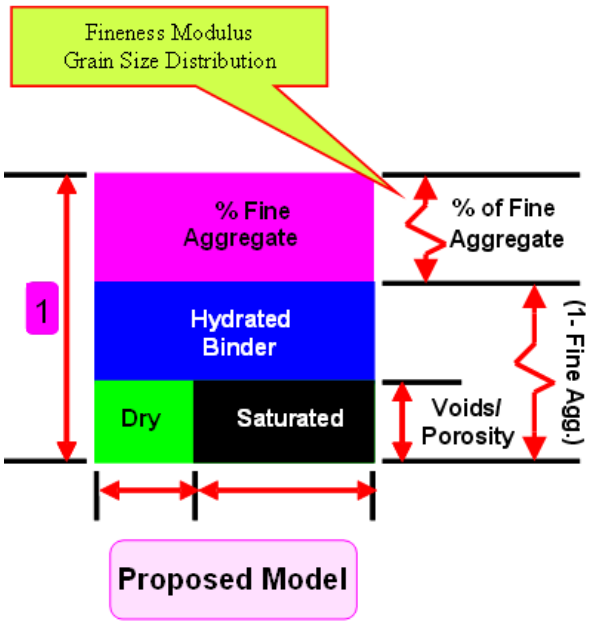

Figure 11. Saturated Area of Concrete Acting as an Electrolyte

In this model the factor 'α_{Vf}' representing the percentage of fine aggregate present in the vicinity of rebar varies from 0 to 1.0 depending on parameters such as fineness modulus of sand, particle size distribution profile of fine aggregate etc. and needs to be further investigated as scope for future research. In this study the value is tentatively taken as 1.0.

5. EXPERIMENTATION

5.1 Materials and Mix Proportions

Ordinary Portland cement (OPC) as per JIS R5210 specifications was used throughout this research. Natural river sand passed through JIS A1102 sieve No. 4 (4.75-mm openings), was used as fine aggregate for all concrete mixes. Its density and water absorption were 2.65 g/cm^3 and 2.21%, respectively. Crushed limestone with a maximum size of 20 mm was used as coarse aggregate with density of 2.70 g/cm^3 and water absorption 0.59%. It was retained on the sieve No.4 (4.75mm-openings) and cleaned before being used. Deformed round carbon steel bars 13 mm in diameter were used as reinforcing steel. The surface of steel bar was polished by sand paper No.200. Finally, steel bar was degreased by acetone just prior to being placed in the mould. The W/C ratio was kept 0.45 with an air content of 3.5±1 %. Mix proportions are shown in the following Table 1.

Table1. Mix proportion

Specimen	W/C	Binder Kg/m^3	Water Kg/m^3	Sand Kg/m^3	Agg. Kg/m^3
Concrete	0.45	386	174	629	1122

5.2 Specimen Preparation and Experiment Scheme

The specimen is derived from the previous research experiment survey (B.H. oh et.al. (2004)) with necessary modifications as explained below in order to take care of the factors that have been overlooked in the past research works. Schematic diagram and

original picture of the prismatic concrete specimen (100x100x400 mm and 100x100x200 mm) with two 13mm diameter steel bars (one bar completely embedded and other coming out from both faces, both having a clear cover of 15mm) cast in steel molds are as shown in Figure 12.

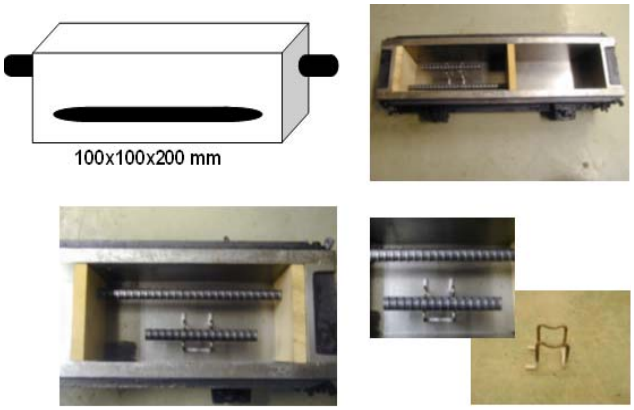

Figure 12. Schematic Diagram of the Specimen

The reason for using two steel bars is to make it possible to measure corrosion potential and corrosion mass loss using the same specimen which is the originality of this experiment scheme. The bar emerging out from the two sides can be used for the corrosion potential measurement only since the two edges are not embedded into the concrete and are not under chloride attack. Therefore, in order to find the mass loss using the same specimen a separate steel bar was embedded completely into the concrete. This was done to obtain more reliable and accurate results. The clear cover was kept 15mm because Uomoto (2000) showed that measured half-cell potential values at concrete surface could be considered as actual value at steel surface, if cover depth was within 20 mm.

The test consists of 24 specimens having a total Cl concentration varying from 0-10 % (NaCl: 0-16.5 % by mass of binder) in mixing water consisting of three sets for 20, 40 and 60°C temperature conditions and 60% relative humidity in environment control chambers. All the specimens were allowed to set and harden in mould for 1 day in controlled sealed curing conditions at 20ºC before being de-moulded. Half-cell potentials were measured with two days interval for all specimens using copper-copper sulfate reference electrode (CSE) in accordance with ASTM C-876 specifications, which can be found elsewhere. For further illustration of the measurement procedure adopted in this research consider the Figure 13. A standard Voltmeter with 0.0001V accuracy is connected with the R.C specimens and the standard electrode through the specified wire in order to make a half-cell potential measuring circuit.

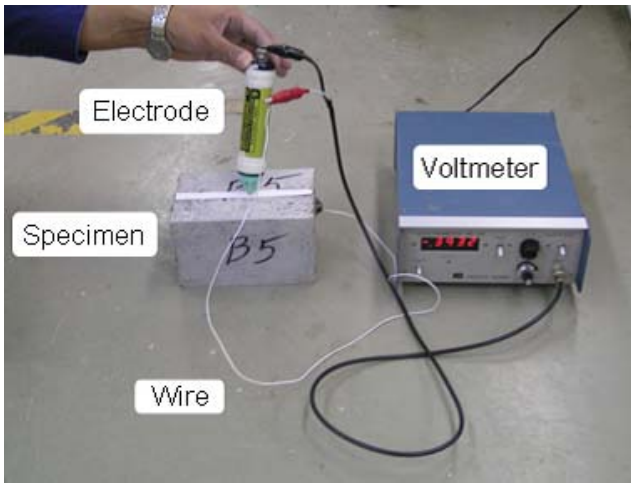

Figure 13. Half-Cell Potential Measurement Assembly

Perhaps one of the most important point in the measurement of half-cell potential is to make the concrete surface wet enough before taking the measurement so that the resistivity of the concrete is reduced to such an extent which does not affect experiment measurement results. If the measured value of half-cell potential does not stop fluctuating during the measurement, it means that surface of the concrete is not wet enough and the resistivity of concrete is hindering the formation of proper contact between the electrode and the concrete electrolyte.

Finally the specimens were split along the position of steel in the concrete and steel bars were removed carefully from the concrete. After the photographic evaluation of the corroded steel reinforcement bars, the corrosion mass loss was determined by gravimetric method after chemical

cleaning of the corrosion products (ASTM G1-03) as shown in Figure 14. Care must be taken that the base metal should not dissolve along with the corrosion products during the chemical cleaning treatment.

Figure 14. Gravimetric Weight Loss Determination Procedure

6. EXPERIMENT RESULTS AND DISCUSSIONS

Figure 15 (a)-(c) & 16 show results of half-cell potential and corrosion rate measurements for ordinary portland cement concrete mixed with 0.0, 0.025, 0.25, 0.6, 1.0, 1.82, 3.65, 6.0, 8.0 & 10.0 percent chloride by mass of binder and three temperature conditions of 20, 40 and 60°C respectively. The half-cell potential values for various cases have a tendency to increase in early age and then approach to certain less variable values but not strictly constant. In general the corrosion potential and the corrosion rate show a non-linear rise with the increase of chloride content and temperature as shown in Figure 15 & 16. But, only in the case of the specimens having the high concentration of Cl and highest temperature show a falling trend and reduction in the corrosion potential values with the increase in temperature. The possible reason could be intensive chloride and high temperature induced corrosion cracking occurred in these specimens. Thus causing the loss of moisture needed for corrosion process and discontinuity of the specimen materials between steel and concrete along the crack face.

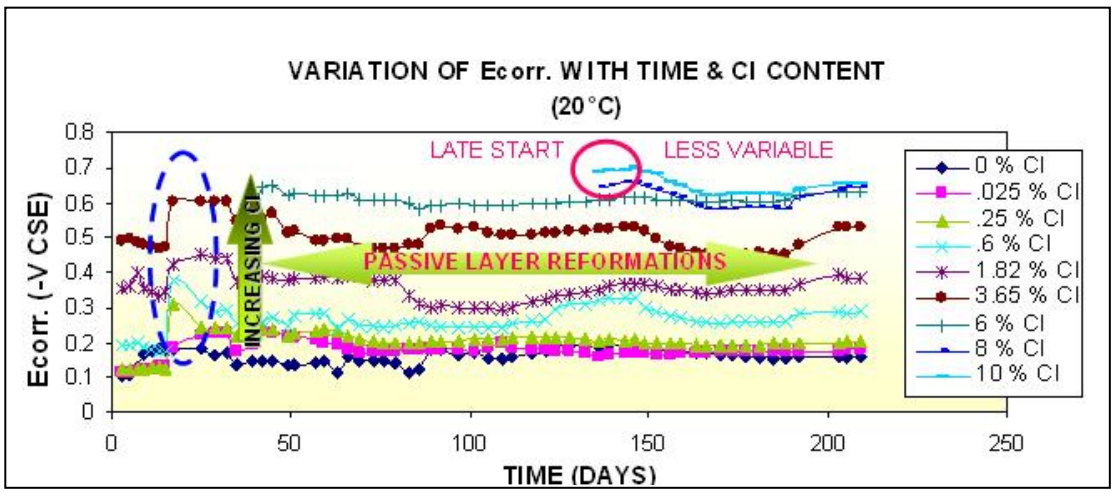

(a)

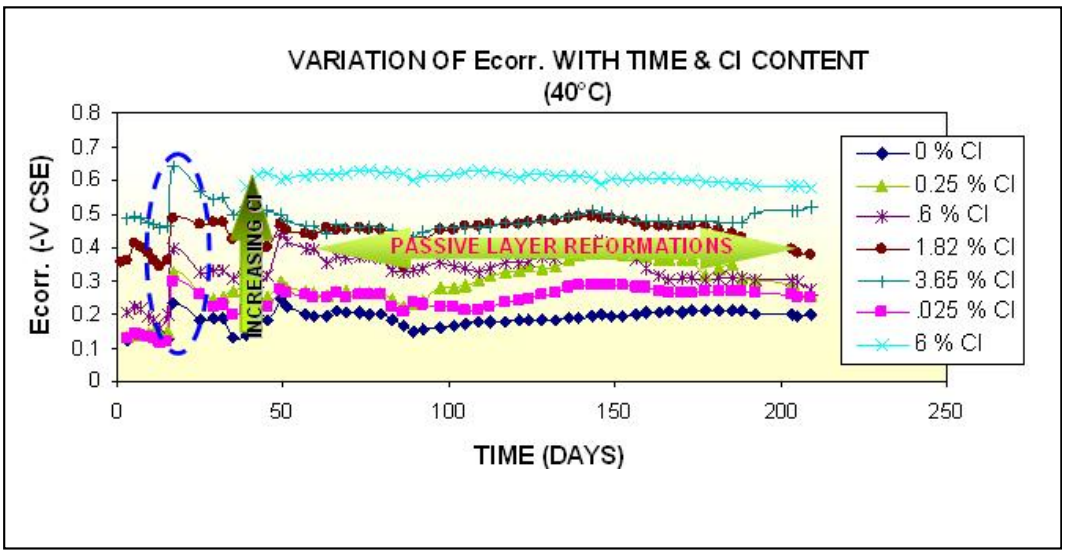

(b)

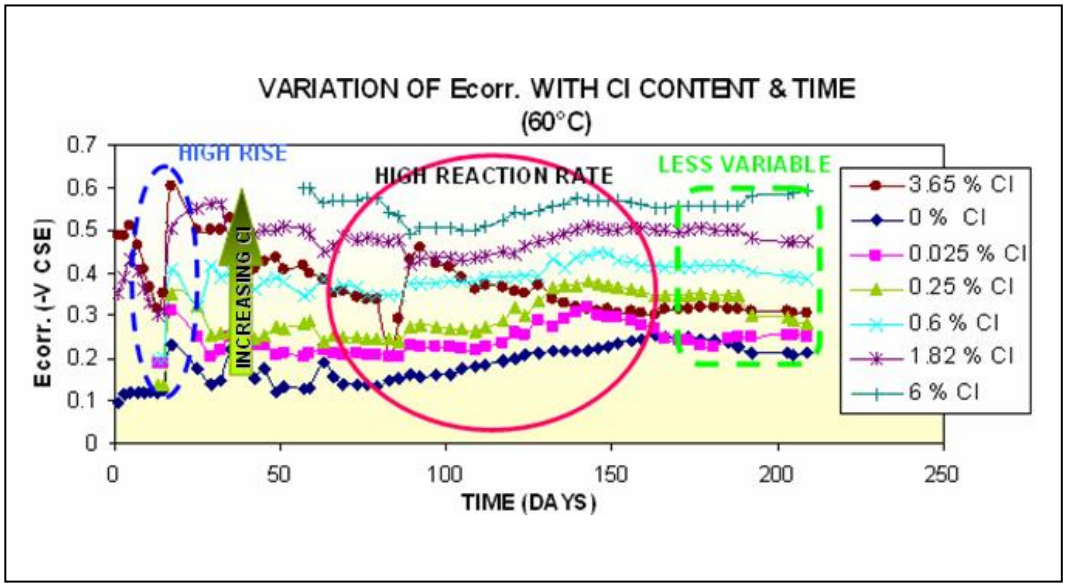

(c)

Figure 15. (a)-(c) Variation of Half-Cell Potential with Age, Cl and Temperature (OPC, W/C=0.45)

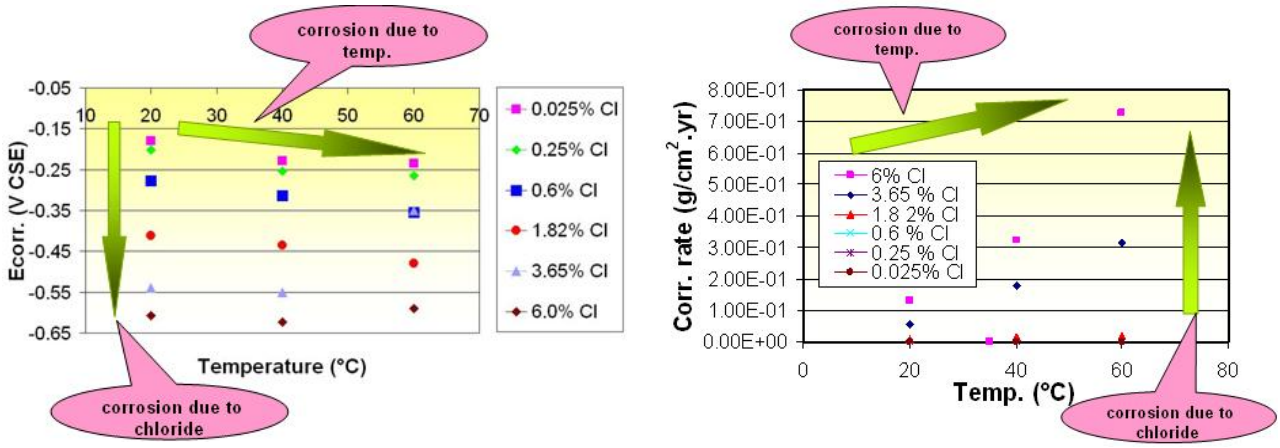

Figure 16. Combined Effect of Chloride and Temperature

7. Verification of Corrosion Potential and Corrosion Rate Model

The corrosion model of DuCOM shows good agreement with the experiment results as shown in Figure 17 & 18 for the effect of chloride on corrosion of steel reinforcement embedded in concrete for both corrosion potential and corrosion current. Thus providing evidence for the efficiency and accuracy of the model. The model though simple but predicts well taking into account influential parameters involved in the process of corrosion in R.C structures. Modeling and verification for the effect of temperature is in the pipeline and will be published soon.

According to ASTM standard C-876, the reinforcement steel bar in concrete is prone to be under the attack of corrosion if the half-cell potential value is below -0.2 Volts. Above that value the steel is in satisfactorily safe condition. The same criterion is also verified by the corrosion model under discussion. In case of chloride induced corrosion, the initiation of corrosion takes place at the threshold value which is mostly considered to be around 0.4% total chlorides by mass of binder and the model under discussion gives a corrosion potential of -0.21 Volts at this value which is just below the value of corrosion potential specified by standards for the detection of initiation of corrosion. Therefore, the corrosion model of DuCOM is also verified by the ASTM Standards in addition to the experimental verification provided in this paper. Hence it can be said that the corrosion model predicts the amount of corrosion both quantitatively and qualitatively with enough accuracy and satisfies the experimental criteria as well as the present scientific theories and standard specifications related to the corrosion of steel reinforcement in concrete structures.

The corrosion model gives the value of corrosion potential 'Ecorr.' in SHE (Standard Hydrogen Electrode) or NHE (Normal Hydrogen Electrode) units. Therefore, in order to compare it with experiment results which are in CSE (Copper-Copper Sulfate Electrode) units, it is necessary to use the standard conversion factor as shown below:

$$CSE\ (V) = SHE\ (V) + 0.316\ V$$

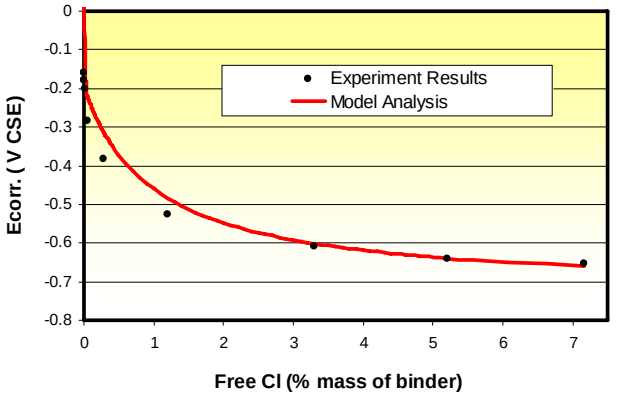

Figure 17. Cl Vs Corrosion Potential Profile (T=20°C, W/C=0.45)

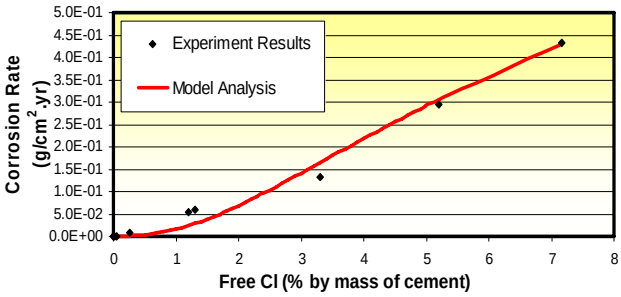

Figure 18. Cl Vs Corrosion Current Profile (T=20°C, W/C=0.45)

8. CONCLUSIONS

The model being in close agreement with the experiment results predicts the corrosion rate and potential with good accuracy and precision. Corrosion in R.C structures increase in a non uniform manner with the severe environmental loadings even at high chloride concentrations in high temperature range. It has been found from the experiment results that the gradient of corrosion profile with temperature becomes significantly steep with the increase in chloride concentration.

Influential parameters on prediction of corrosion in RC structures involving the severe environmental loadings are experimentally determined and numerically discussed through parametric study. Appropriate parameters for material modeling of corrosion on the basis of already developed computational scheme (Ishida, T., 1999a) are successfully identified.

9. REFERENCES

Nishida, N.Otsuki, M.A, Baccay & J. Hamamoto. (2005) Temperature Dependency of corrosion rate of steel bars in concrete influenced by material segregation, *Tokyo Institute of Technology, Japan, Toa Corporation, Japan.*

Ishida, T. (1999a) An integrated computational system of mass/energy generation, transport and mechanics of materials and structures, *Thesis (PhD), University of Tokyo.*

Koichi Maekawa, Tetsuya Ishida and Toshiharu Kishi, "Multi-scale Modeling of Concrete performrmance". *Journal of Advanced Concrete Technology; Vol. 1, No. 2, 2003, pp. 91- 126.*

J. Tafel, *Zeitschrift für Eleckrochemie* 1906, *12*, 112-122 (In german)

Uomoto, T., 2000, Non-destructive Testing in Civil Engineering, *Elsevier, pp.671-678.*

Byung Hwan Oh, Bong Seok Jang and Seong Cheol Lee, Chloride diffusion and 11corrosion initiation time of reinforced concrete structures, *Proceedings of the 11international workshop on Microstructure and Durability, Sapporo, Japan, Feb. 2004.*

Ho Thi Lan Anh, "Modeling of chloride transport under arbitrary temperature", *Master Thesis, University of Tokyo, 2005*

ASTM C 876-91, 1999, *Standard Test Method for Half-Cell Potentials of Uncoated Reinforcing Steel in Concrete,* ASTM, U.S.A.

ASTM G1-03, 2002, *Standard test practice for preparing, cleaning and evaluating corrosion test specimens,* ASTM, U.S.A.

T. Ishida and Raja Rizwan HUSSAIN (2005) Coupled Effect of Chloride and Temperature on the corrosion of R.C Structures based on thermodynamic approach, *The Tenth East Asia-Pacific Conference on Structural Engineering and Construction (EASEC-10),* Bangkok, Thailand.

BS 8110, Structural use of concrete, *Code of Practice for design and construction,* 1997.

ACI 222R-96, (2001) *Corrosion of Materials in concrete.*

Evertte and Treadaway (1983) "Pore solution composition and chloride binding capacity of silica fume cement pastes". *Journal of Materials and Structures,Vol. 16, No.1, pp 19-25.*

John P. Broomfield., "Corrosion of Steel in Concrete", Chapter 6, *Electrochemical repair techniques,* E and FN SPON, London, 1997.

G.K Glass, C.L Page and N.R Short, "Factors affecting the corrosion rate of steel in carbonated mortars", *Corrosion Science, Vol.32, No.12, p.p 1283-1294, 1991.*

M. Raupach, (1996) "Investigation of the influence of oxygen on corrosion of steel in concrete" Part I and II". *Journal of Materials and Structrues, Vol.29, NO. 3, pp.174-184. and Vol. 29, No. 4, pp. 226-232.*